

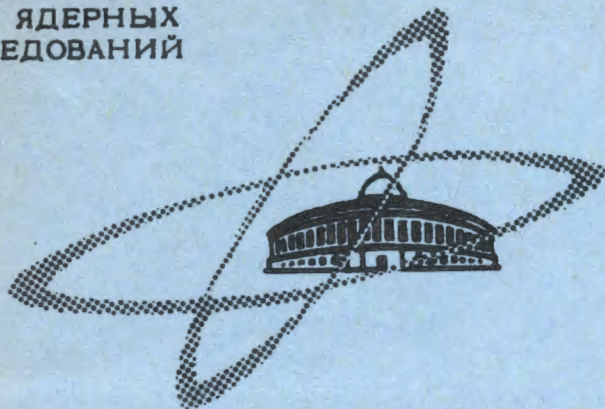
A-99

Phys. Lett., 1967, v. 24B, N7,
p. 348-352

ОБЪЕДИНЕННЫЙ
ИНСТИТУТ
ЯДЕРНЫХ
ИССЛЕДОВАНИЙ

Дубна

E1 - 3148



ЛАБОРАТОРИЯ ВЫСОКИХ ЭНЕРГИЙ

M.A. Azimov, A.M. Baldin, A.S. Belousov ,
J. Hladký , L.I. Zhuravleva, G.A. Ososkov,
J. Manca , A.T. Matyushin, V.T. Matyushin,
R. Firkowski , M.N. Khachatryan,
M.S. Khvastunov, I.V. Chuvilo, L.N. Shtarkov

OBSERVATION OF THE $(e^+ e^-)$ - DECAY
MODES OF NEUTRAL VECTOR MESONS

1967.

4795/3 48

M.A. Azimov, A.M. Baldin, A.S. Belousov*,
J. Hladký**, L.I. Zhuravleva, G.A. Ososkov,
J. Manca***, A.T. Matyushin, V.T. Matyushin,
R. Firkowski****, M.N. Khachatryan,
M.S. Khvastunov, I.V. Chuvilo, L.N. Shtarkov*

OBSERVATION OF THE $(e^+ e^-)$ - DECAY
MODES OF NEUTRAL VECTOR MESONS

Submitted to ЯФ
Phys.Let.

* P.N. Lebedev Physics Institute, Moscow, USSR.

** Physical Institute of the Czechoslovak Academy of Sciences,
Praha, Czechoslovakia.

*** Electrotechnical Institute of the Slovak Academy of Sciences,
Bratislava, Czechoslovakia.

**** Institute for Nuclear Research, Łódź, Poland.

Introduction

The importance of the experimental determination of the partial widths of the $V \rightarrow e^+e^-$ decays (1) of vector mesons has been stressed several times^[1-5]. These decay probabilities are related to the important problems of strong and electromagnetic interactions. However, despite some attempts to experimentally determine e^+e^- decay rates^[6-10] we have only the evaluations of the upper limits of these probabilities.

The difficulty to observe the above decays is due to the fact that they are very rare (at least of the order of magnitude of 10^{-4} of the basic decay mode). This circumstance makes it necessary to separate the effect from the large number of imitating processes among which pion production is of importance.

In our experiment in order to separate e^+e^- decays a new method has been used of jointly operating spark chambers and Čerenkov gamma-spectrometers^[11,14]. The advantages of this method are as follows:

- 1) A possibility to measure both the angles of particle emergence and their energies, and, hence, to calculate the effective mass of the resonance.
- 2) High apparatus sensitivity to particles of the shower origin (photons and electrons).
- 3) A possibility to simultaneously detect the processes $V \rightarrow e^+e^-$, $V \rightarrow \gamma\gamma$ and $V \rightarrow \pi^0\gamma$ in a wide range of effective masses, which allows to safely measure relative decay rates.

The measurement of the processes $V \rightarrow \pi^0\gamma$ is of special interest and besides allows to safely determine quantitatively the relative probabilities of electron decays of vector mesons. Strictly speaking, the matter is that in our experiments the differential cross section of the process:

$$\pi^- + p \rightarrow e^+ + e^- + n$$

is measured. In order to determine the partial width of the $V \rightarrow e^+e^-$ decay using the value of this cross section the experimental data are necessary not only on the differential cross section of vector meson production

but also on its density matrix. Unfortunately, the available data are not complete. The measurement of the process $V \rightarrow \pi^0 \gamma$ simultaneously with the process $V \rightarrow e^+ e^-$ eliminates this difficulty since the angular distributions of these processes coincide to an accuracy of 10^{-6} (see Appendix I).

This note reports on the first run as a result of which $e^+ e^-$ pair production cross sections have been measured in the reactions

$$n + \omega \rightarrow n + e^+ + e^- \quad (2a)$$

$$\pi^- + p \rightarrow n + \rho \rightarrow n + e^+ + e^- \quad (2b)$$

$$n + \phi \rightarrow n + e^+ + e^- \quad (2c)$$

and on the evaluation of the relative decay rates of the lepton decays of vector particles. Data on the study of $V \rightarrow \pi^0 \gamma$ process are under treatment and will be published later.

2. Description of Experimental Apparatus

Vector mesons were produced by 4.0 GeV/c pions ($\Delta p/p = \pm 1.5\%$) in a liquid hydrogen target 50 cm long in reaction (2). In order to separate lepton decays use was made of a two-channel system of jointly operating spark chambers and Cerenkov total absorption gamma-spectrometers.

For each event this system makes it possible to measure three parameters: the energies E_1 and E_2 of electrons produced as a result of the vector particle decay and the opening angle (θ) between them. The knowledge of the above three parameters allows to calculate the effective mass of the event^{14/}.

A schematic view of the experimental geometry and apparatus is shown in Fig. 1. Scintillation counters S_1 and S_2 serve to monitor the incident particle beam. Spark chambers in each of two identical chan-

nels are a system of four modules of the $50 \times 50 \text{ cm}^2$ fiducial area each and a 10 cm discharge gap. For conversion of particles of the shower origin brass plates of the total thickness of 1.2 (0.4x3) rad. units are placed in front of the second and subsequent chambers.

In order to increase the triggering efficiency of the spark chamber system the counters S_3 and S_4 $50 \times 50 \text{ cm}^2$ large and 2 cm thick are put between the counters and the Cerenkov gamma-spectrometers.

Lead glass of high transparency $50 \times 50 \times 30 \text{ cm}^3$ and $50 \times 50 \times 20 \text{ cm}^3$ large, respectively, is used as radiator material in Cerenkov gamma-spectrometers. In order to collect Cerenkov light use is made of nine photomultipliers having a 17 cm photocathode diameter.

The system of spark chambers is triggered by the $S_1 S_2 S_3 S_4 C_1 C_2$ coincidences if

$$1) E_1 > E_1^0 ; 2) E_2 > E_2^0 ; 3) E \equiv E_1 + E_2 > E^0 .$$

From the kinematic analysis of the process the account of the energy resolution of γ -spectrometers in our experiment the threshold values have been found : $E_1^0 = E_2^0 = 0,5 \text{ GeV}$ and $E^0 = 3 \text{ GeV}$. The optimal experimental arrangement is found from the kinematic analysis of reactions (2) and corresponds to geometry when the direction of electron emergence at a minimum angle is near the detector axes. In this geometry the device is most sensitive to peripheral interactions when the momentum transferred to the nucleon is small. The optimal geometry and the curve of efficiency dependence upon the values of the momentum transfer have been calculated by using the electronic computer. The analysis of energy spectra of decay electrons from processes (2) in the optimal geometry shows that within solid angles viewed by detectors, electron energy spectra in each channel have the maximum at $E_1 = E_2 \approx \frac{E_\pi^-}{2}$, where E_π^- - is the energy of the incident particle. It is evident that another condition also holds; namely, the energy sum $E_1 + E_2$ equals the energy of the incident pion to an accuracy of the nucleon momentum transfer. The above conditions allow to use in measurements the logic system for selecting events of interest and thus, to considerably reduce the background.

3. Calibration

Cerenkov gamma-spectrometers were calibrated with an electron beam in the energy range from 1.5 to 4 GeV. Spectrometers operate linearly in this energy range the energy resolution being about $\pm 5-7\%$. For effective mass calibration of the apparatus on $\eta + \gamma\gamma$ and $\omega + \pi^0\gamma$ decays were used which had been obtained simultaneously in the same experiment.

4. Experimental Procedure

The total number of negative pions passed through a liquid hydrogen target during the runs was about $3 \cdot 10^9$. We took 20000 pictures of the spark chambers. From these pictures 46 were selected having a single, and only single, track of the charged particle in the 1-st and 2-nd channels.

There is pronounced peak with a centre at the energy equal to that of incident pions and the halfwidth at the halfmaximum of about 0,3 GeV in the $E_1 + E_2$ energy distribution for 46 events. This agrees with the energy resolution of the gamma-spectrometers calculated from the resolving power of the Cerenkov spectrometer used. Hence, in the experimental conditions, the decays of meson produced in peripheral π^-p interactions were mainly detected. Only events of the total energy $(4 \pm 0,4)$ GeV (25 events) were included in the final list of (e^+e^-) events, which corresponds to the interval of two standard deviations.

The distribution for 25 candidates on the opening angle $\theta_{1,2}$ (Fig.3) has its maximum at the minimum angle for two-particle decays of ρ^- and ω -mesons at 4 GeV: $\theta_{\min} = 2 \arcsin(m/E)$. This shows that the apparatus detected, mainly, ρ^- and ω -mesons. The events at angles smaller than 20° are due to the gamma-gamma conversion in the liquid hydrogen target and spark chamber walls. The quantitative evaluations of the conversion will be given below. Here we note that events having the opening angle larger than 20° ($\theta_{\min} \cong 22^\circ$ for ρ^- - and

ω -mesons) should be included in the final list of events, if selection by two standard deviations is used for the accuracy of determining the angle in the experiment.

The distribution for 25 candidates on the effective mass

$$M(e^+e^-) = \sqrt{2 E_1 \cdot E_2 (1 - \cos \theta(e^+e^-))} \quad (3)$$

is shown in Fig. 4a. It shows, the same as the opening angle distribution, events having ρ and ω masses and the admixture of events having masses in the interval from 450 to 650 MeV.

The distribution for events selected from 25 was plotted in Fig. 4b using the above criteria: $E(V) = (4.0 \pm 0.4)$ GeV, the opening angle

$\theta(e^+e^-) > 20^\circ$. Thus, 19 events were selected. Naturally, the peak in the ω and ρ -meson interval in this Fig. 4b is seen much better. One event in the 1100 MeV mass interval can be identified as the $\phi \rightarrow e^+e^-$ decay. Solid curves in Figs. 3 and 4 are theoretical distributions calculated by the Monte-Carlo method for the $\omega \rightarrow e^+e^-$ decays. In the calculation use was made of the values of the mass $M(\omega) = 783$ MeV and the width $\Gamma(\omega) = 0$ and the dependence of the differential cross section of ω -meson production from t (the square of the four-momentum transfer) approximated by the expression^{/21/}:

$$d\sigma/dt = \exp(4t) . \quad (4)$$

The kinematical selection for the $V \rightarrow e^+e^-$ events is shown in Fig. 5. Each event from 25 is shown in this figure by a point at the plane where along the ordinate axes there is the energy ratio for two decay particles, E_{e_1} / E_{e_2} , whereas along the absciss there is an opening angle. Curves 2 and 3 are theoretical ones calculated for the $\rho \rightarrow e^+e^-$ and $\omega \rightarrow e^+e^-$ decays at 4 GeV π^- -meson energy. Curves 1 and 4 are boundaries for the position of curves 2 and 3 corresponding to two standard deviations from the energy and angle resolutions of the apparatus. As is seen from the Fig. 5, in the interval two standard deviations wide there are 13 events which were identified as ρ - and ω -

meson decays into the (e^+e^-) pairs. One event was identified as the $\phi \rightarrow e^+e^-$ decay. The events strictly identified as (e^+e^-) decays of ρ^- , ω^- and ϕ^- mesons are shaded in Figs. 2-4. As possible background sources the following processes were considered:

1. Simulation of e^+e^- events by $\pi\pi^-$ -pairs. A special run was carried out in order to clarify possible $\pi\pi^-$ -pair contribution. The obtained data show that the probability of electron simulation by the pion, under the condition that they have an equal momentum, does not exceed $5 \cdot 10^{-4}$, hence, for the overall system this probability is not larger than $2.5 \cdot 10^{-7}$.

2. The reactions of e^+e^- -pair production in π^-p -interactions avoiding resonance states in the e^+e^- system (including Dalitz pairs, i.e. the decay modes $\omega \rightarrow \pi^0 e^+e^-$ or $\pi^0 \rightarrow \gamma e^+e^-$). As is shown in Appendix III, the contribution of these pairs is negligibly small, if e^+e^- -pairs having the effective mass $M \geq 0.5$ GeV are detected.

3. Conversion due to gamma-gamma events in the spark-chamber walls and in the target. In order to determine the values of the conversion background the experimental data on gamma-gamma events obtained simultaneously with the data on e^+e^- -events were used. Gamma-gamma events were selected according the criteria analogous to that which were employed in selecting e^+e^- -events. The evaluations show that the value of the conversion background in the mass interval from 450 to 650 MeV is 5 events, whereas in the mass interval from 650 to 950 MeV it does not exceed 1.4 event, which is about 10% of the number of (e^+e^-) events identified as vector particle decays.

5. Experimental Results

Since in the experiment the differential cross section of processes (2) were measured in some angle region, then in treating the data it is necessary to take into account angular distributions both of vector particle production and decay.

As is shown in Appendix II, the cross section of processes (2) can be written as

$$\sigma = d\sigma_v \cdot d\Omega_q \cdot \frac{\Gamma_a}{\Gamma} \cdot \frac{3}{4\pi} \cdot \frac{1}{2} |1 - W_{00}(\theta^*, \Phi)| \cdot f(m^2) dm^2 \quad (5)$$

where $d\sigma_v$ is the cross section of vector particle production, Γ_a / Γ the value measured in the present experiment, $\frac{3}{4\pi} \cdot \frac{1}{2} |1 - W_{00}(\theta^*, \Phi)| d\Omega_q$ is the angular distribution of e^+e^- decay products in the vector particle rest system. The coordinate axes are taken so that the z axis is directed along the pion beam, whereas the y axis is going along the normal to the reaction plane, $f(m^2) dm^2$ is the mass distribution of the unstable particle. The fact that in the experiment the cross sections of the processes $V \rightarrow e^+e^-$ and $V \rightarrow \pi^0\gamma$ are measured simultaneously, all the factors in formula (5) are similar (except for Γ_a), allows to exclude unknown factors and determine the ratio $\frac{\Gamma_{e^+e^-}}{\Gamma_{\pi^0\gamma}}$ by using the ratio of the above cross sections. However, the data on the $V \rightarrow \pi^0\gamma$ process have not been treated. Therefore, the values $d\sigma_v$ and $W_{00}(\theta^*, \Phi)$ taken from the literature^[12,13,19] were substituted to formula (5). The angular distributions of vector mesons in reactions (2) were taken in the form of (4). At present the data on the ω -meson production density matrix are most uncertain. As far as ρ - and ω -meson production density matrix is concerned, $\rho_{00} = 0.5-0.8$ ^[17] whereas ρ_{10} and ρ_{1-1} are small (≤ 0.1). It can be shown that for our geometry the above information is sufficient to obtain required evaluations. Indeed, in the experiment, the angle θ^* has the values in the interval from $70^\circ-110^\circ$. In this angle region and the uncertainty interval of the density matrices the expression $\frac{3}{2} |1 - W_{00}(\theta^*, \Phi)|$ is varied within $1 \leq \frac{3}{2} |1 - W_{00}(\theta^*, \Phi)| \leq 1.3$.

Our experimental data can be given as follows:

$$\frac{\Gamma(\rho \rightarrow e^+e^-)}{\Gamma(\rho)} \cdot \sigma_t(\rho) + \frac{\Gamma(\omega \rightarrow e^+e^-)}{\Gamma(\omega)} \cdot \sigma_t(\omega) = (0.45 \pm 0.12) \cdot 10^{-4} \text{ mb} \quad (6)$$

$$\frac{\Gamma(\phi \rightarrow e^+e^-)}{\Gamma(\phi)} \cdot \sigma_t(\phi) \leq 1.8 \cdot 10^{-5} \text{ mb} \quad (7)$$

In such a form they do not depend on the data of other experiments and certain physical suggestions. Assume that electromagnetic current is transformed according to the octet representation of SU(3) and let $\theta = 38^\circ$ for the ω - ϕ mixing angle. Corrections for the SU(3) symmetry violation are introduced using the linear dependence $\Gamma(V \rightarrow e^+ e^-)$ on the vector particle mass^[3].

For the cross sections $\sigma_t(\rho)$, $\sigma_t(\omega)$ and $\sigma_t(\phi)$ the following data^[19,12] are used:

$$\sigma_t(\rho) = (0.75 \pm 0.13) \text{ mb}$$

$$\sigma_t(\omega) = (0.34 \pm 0.07) \text{ mb}$$

$$\sigma_t(\phi) = (0.009 \pm 0.005) \text{ mb} .$$

Under these assumptions from (6) and (7) one can make two independent evaluations of the important physical parameter: the width of the vector meson octet decay into e^+ and e^- :

$$\Gamma(V_8 \rightarrow e^+ e^-) = (0.45 \pm 0.14) \cdot 10^{-2} \text{ MeV} \quad (8)$$

$$\Gamma(V_8 \rightarrow e^+ e^-) \leq 2.6 \cdot 10^{-2} \text{ MeV} \quad (9)$$

As is seen, both the evaluations are in agreement. The evaluations correspond to the following ratios:

$$\frac{\Gamma(\rho \rightarrow e^+ e^-)}{\Gamma(\rho)} = (0.39 \pm 0.12) \cdot 10^{-4}$$

$$\frac{\Gamma(\omega \rightarrow e^+ e^-)}{\Gamma(\omega)} = (0.48 \pm 0.15) \cdot 10^{-4}$$

$$\frac{\Gamma(\phi \rightarrow e^+ e^-)}{\Gamma(\phi)} \leq 2 \cdot 10^{-8}$$

In order to compare the width $\Gamma(V_8 \rightarrow e^+ e^-)$ with indirect estimates let us express it by the $V - \gamma$ -interaction constant: $g_{\nu\gamma} m_\nu^2 \phi_\mu A^\mu$ which is of importance for electromagnetic processes. Here m_ν is vector particle mass, ϕ_μ is the operator of the meson field, A^μ is the vector-potential of the electromagnetic field.

Calculation provides $\Gamma(\rho \rightarrow e^+ e^-) \approx \frac{1}{4} g_{\rho\gamma}^2 \cdot \frac{e^2}{4\pi} \cdot \frac{1}{3}$. And from (8) we find:

$$g_{\rho\gamma}^2 = (0,24 \pm 0,11) \cdot \alpha$$

where α is the fine structure constant. If one assumes that the electromagnetic structure of the pion is completely due to the ρ -meson, the charge of the pion is expressed using $g_{\rho\gamma}$ as follows: $e^2 = g_{\rho\gamma}^2 \cdot f_{\rho\pi\pi}^2$. If $f_{\rho\pi\pi}^2$ is taken from the $\rho \rightarrow 2\pi$ decay width, $g_{\rho\gamma}^2 = 0,42 \cdot \alpha$. Recently an evaluation was made^[15] of the same constant from the ρ -meson photoproduction cross section at small angles and the following value was found: $g_{\rho\gamma}^2 = 0,24 \cdot \alpha \cdot (1 \pm 0,3)$. Thus, our evaluation of the $\Gamma(\rho \rightarrow e^+ e^-)$ width within experimental errors agrees with indirect evaluations.

Note: The basic data of the present investigation were reported at the XIII International Conference on High Energy Physics, Berkeley. Recently A. Wehmann et al.^[20] have measured the ratio

$\frac{\Gamma(\rho \rightarrow \mu^+ \mu^-)}{\Gamma(\rho \rightarrow 2\pi)} = (4,3 \pm 1,4) \cdot 10^{-5}$. This value has been obtained under the assumption that the ω -meson contribution is negligibly small and agrees with our data within experimental errors.

The authors wish to express their thanks to the proton synchrotron staff for excellent accelerator operation during the experiment, V.S.Pantuyev, B.Zelenov for taking part in the apparatus adjustment and in measurements, V.Ivanov, V.Arkipov and V.Prokhorov for help in preparing and running the experiment, E.Maltsev and V.Komolova for preparing the computer programmes.

We gratefully acknowledge the continuous interest of P.A.Cerenkov, a correspondent-member of the USSR Academy of Sciences, Prof.M.I.Podgoretsky and Dr. V.A.Sviridov for helpful discussions.

APPENDIX I

Angular Distributions of the Processes

$$V^0 \rightarrow e^+ + e^- \quad \text{and} \quad V^0 \rightarrow \pi^0 + \gamma$$

Let us take the density matrix $\langle m | \rho | m' \rangle$ in the vector particle rest system: λ_a and λ_b are spiralities of the decay particles. Using the methods of refs. ^[16,17] for the angular distribution of the two-particle decay we have:

$$W_1(\theta^*, \Phi) = N' \sum_{\lambda_a \lambda_b} |A(\lambda_a, \lambda_b)|^2 e^{i(m-m')\Phi} \Phi_{d_{M\Lambda}}^1(\theta^*) d_{M\Lambda}^1(\theta^*) \langle m | \rho | m' \rangle \quad (I.1)$$

N' is normalization, $\Lambda = \lambda_a - \lambda_b$ are coordinate axes taken according to Fig. 6.

According to the requirements of the Hermitian character $\rho, S_p \rho = 1$ and from the symmetry condition $\langle m | \rho | m' \rangle = (-1)^{m-m'} \langle -m | \rho | -m' \rangle$ (the invariance with respect to reflection) we have the usual parametrization $\langle m | \rho | m' \rangle$:

$$\begin{array}{ccc} \rho_{11} & \rho_{10} & \rho_{1-1} \\ \rho_{10}^* & 1-2\rho_{11} & -\rho_{10}^* \\ \rho_{1-1} & -\rho_{10} & \rho_{11} \end{array} \quad \rho_{00} = 1 - 2\rho_{11}^* \rho_{11} - \rho_{1-1} \quad \begin{array}{l} \text{are real} \\ \text{numbers} \end{array}$$

Consider the process $V^0 \rightarrow P + \gamma$. In this case $\lambda_a = 0$, $\lambda_b = \pm 1$. From invariance with respect to space reflection we find:

$$A(0, +1) = -A(0, -1).$$

Thus, the angular distribution is expressed only by one dynamic parameter describing the decay. From I.1 we obtain

$$W_{10}(\theta^*, \Phi) = \frac{1}{2} [1 - W_{00}(\theta^*, \Phi)] \frac{3}{4\pi} \Gamma_{p\gamma} \quad (I.2)$$

where
$$W_{00} = \rho_{00} \cos^2 \theta^* + \rho_{11} \sin^2 \theta^* - \rho_{1-1} \sin^2 \theta^* \cos 2\Phi - \sqrt{2} \operatorname{Re} \rho_{10} \sin 2\theta^* \cos \Phi \quad (I.3)$$

coincides with the angular distribution of the $V^0 \rightarrow P + P$ decay.

$\Gamma_{py} = 2|A(0+1)|^2$ is the width of the $V^0 \rightarrow P + \gamma$ decay.

Consider the $V^0 \rightarrow e^+ + e^-$ decay. In this case $\lambda_a = \pm 1/2$, $\lambda_b = \pm 1/2$ and the invariance requirement with respect to the reflection gives

$$|A(+\frac{1}{2}, +\frac{1}{2})|^2 = |A(-\frac{1}{2}, -\frac{1}{2})|^2; \quad |A(+\frac{1}{2}, -\frac{1}{2})|^2 = |A(-\frac{1}{2}, +\frac{1}{2})|^2.$$

Thus, the angular distribution of the decay is expressed with two independent parameters. Using (I.1) and the real form of d -functions it is easy to find:

$$W_{\frac{1}{2} \frac{1}{2}}(\theta^*, \Phi) = 2[|A(+\frac{1}{2}, +\frac{1}{2})|^2 W_{00}(\theta^*, \Phi) + |A(+\frac{1}{2}, -\frac{1}{2})|^2 W_{10}(\theta^*, \Phi)] \quad (I.4)$$

Expression (I.4) is a consequence of the momentum and parity conservation laws only. Using the fact that a fraction of the process is described by quantum electrodynamics, show that the first term is always smaller than the second one.

The amplitude $\langle p \lambda_a \lambda_b | A | 1m \rangle$ should be of the form (singlephoton approximation)

$$\langle p \lambda_a \lambda_b | j_\mu | 0 \rangle = \frac{e^2}{q^2} \langle 0 | J_\mu | 1m \rangle, \quad (I.5)$$

where

$$\langle \vec{p} \lambda_a \lambda_b | j^\mu | 0 \rangle = \bar{u}_\lambda(p') \gamma_\mu v_\lambda(p) \delta(\vec{p}' + \vec{p}) = \bar{u}_{-\lambda}(\vec{p}) e^{i\pi S_2} \gamma_\mu v_\lambda(p) \delta(\vec{p}' + \vec{p})$$

γ_μ ; u_λ , v_λ are Dirac matrices and spinors, J_μ - hadron current S_2 is an operator of the momentum projection at the $\downarrow \vec{p}$ axis. In order to find the amplitudes of interest matrix element (I.5) should be transformed into the total momentum representation

$$A(+\frac{1}{2}, \pm \frac{1}{2}) = \frac{e^2}{q^2} \langle 0 | J | 1 \rangle \sum_m \int \langle m, \frac{1}{2} \pm \frac{1}{2} | \vec{p}' \pm \frac{1}{2} \pm \frac{1}{2} \rangle \bar{u}_+(\vec{p}) e^{i\pi S_2} \gamma_\mu v_\pm(\vec{p}) d\Omega. \quad (I.6)$$

Here $\langle 0 | J_\mu | 1m \rangle = \langle 0 | | J | | 1 \rangle \delta_{Mm}$ is used. Calculation (1.6) provides:

$$|A(-\frac{1}{2}, +\frac{1}{2})|^2 = 2 \left(\frac{m_e}{m_V} \right)^2 |A(-\frac{1}{2}, -\frac{1}{2})|^2, \quad (1.7)$$

where m_e is electron mass, m_V is vector particle mass. Comparing (1.7), (1.4) and (1.2) one can see that the angular distributions of the processes $V^0 \rightarrow e^+ + e^-$ and $V^0 \rightarrow \pi^0 + \gamma$ coincide to an accuracy of many orders of magnitude exceeding that of the present day experiment.

APPENDIX II

The differential cross section of the reactions

$$e^+ + e^- + n \quad (II.1)$$

$$\pi^- + p \rightarrow$$

$$\pi^0 + \gamma + n \quad (II.2)$$

are of the form

$$d\sigma = \frac{4\pi}{VE_\pi E_p} \frac{1}{2} \frac{d^3 P_1}{E_1} \frac{d^3 P_2}{E_2} \frac{d^3 P_3}{E_3} \delta(P_1 + P_2 + P_3 - P_\pi - P_p) \sum_{\lambda_1 \lambda_2 \lambda_3} |\langle \lambda_1 P_1 \lambda_2 \times \lambda_3 P_3 | M | \lambda_p P_p \lambda_\pi P_\pi \rangle|^2, \quad (II.3)$$

where P_π, P_p, E_π, E_p are momenta and energies of initial particles, V is their relative velocity, $P_1, P_2, P_3, E_1, E_2, E_3$ are three-dimensional momenta and energies of residual particles, $\lambda_1, \lambda_2, \lambda_3$ are spiralities of residual particles, λ_p is proton spirality, $\langle M \rangle$ is an invariant matrix element.

Reactions (II.1) and (II.2) will be considered as going in two stages:

I. Production of the unstable particle V ; II. The V particle decay.

The kinematics of these processes is especially simple when the first stage is considered in the $\pi^- p$ c.m.s., whereas the decay is considered in the V -particle rest system. In this connection introduce the summed momentum of particles 1 and 2 (the V particle momentum) $t = P_1 + P_2$ and the momentum $\vec{q} = \frac{1}{2}(P_1 - P_2)$ and transform the invariant phase space as follows:

$$\begin{aligned} & \frac{d^3 P_1}{E_1} \frac{d^3 P_2}{E_2} \frac{d^3 P_3}{E_3} \delta(t + P_3 - P_\pi - P_p) = \\ & = \left[\frac{d^3 t}{t_0} \frac{d^3 P_3}{E_3} \delta^4(t + P_3 - P_\pi - P_p) \right] \left[\frac{t_0 d^3 \vec{q}}{E_1 E_2} \right]. \end{aligned} \quad (II.4)$$

Since the first factor is relativistically invariant, the second factor is also invariant and they can be considered in different coordinate systems. In the system where $t = 0$ (the V -particle rest system) the second factor is of the form:

$$\frac{m}{\sqrt{m_1^2 + q^2} \sqrt{m_2^2 + q^2}} q^2 dq d\Omega \quad ,$$

where $m = \sqrt{m_1^2 + q^2} + \sqrt{m_2^2 + q^2}$ is the V particle mass by definition. Passing from the variable q to the variable m , we have for the phase space:

$$\frac{d^3 P_3}{E_3} \frac{d^3 t}{t_0} \delta^4 [t + P_3 - P_\pi - P_p] q \frac{dm^2}{2m} d\Omega_q \quad . \quad (II.5)$$

If the V particle is considered to be stable, the invariant matrix element contains the factor $\delta(m^2 - m_2^2)$ and the integration over the effective mass is of formal importance. If according to the same experimental conditions it is necessary to take into account the final resonance width, then instead of the δ -function the distribution^{18/} is introduced of the type:

$$\frac{1}{\pi} \frac{\Gamma(m)}{(m^2 - m_2^2)^2 + \Gamma^2(m)} \quad . \quad (II.6)$$

Invariant factor (II.6) can be considered as a part of the propagator correlating the production and the decay of the unstable particle. The matrix element M should be given as the sum of the products of invariant co-factors:

$$\begin{aligned} \langle \lambda_1 P_1 \lambda_2 P_2 \lambda_3 P_3 \alpha | M' | \lambda_p P_p P_\pi \rangle &= \sum_{\lambda_\nu} \langle \lambda_1 P_1 \lambda_2 P_2 \alpha | A | t \lambda_\nu J_\nu \rangle \times \\ &\times \langle t \lambda_\nu J_\nu P_3 \lambda_3 | R | \lambda_p P_p P_\pi \rangle \end{aligned}$$

here $\langle \lambda_1 P_1 \lambda_2 P_2 \alpha | A | t \lambda_\nu J_\nu \rangle$ is the decay amplitude, J_ν is the unstable particle spin, λ_ν is its spirality, alpha numerates the decay channel, $\langle t \lambda_\nu J_\nu P_3 \lambda_3 | R | \lambda_p P_p P_\pi \rangle$ is the reaction amplitude. The strike of M means that M' differs from M by a factor type (II.6). Now use relativistic invariance and write A in the rest system of the V particle:

$$\langle \lambda_1 \vec{P}_1 \lambda_2 \vec{P} \alpha | A | t \vec{J}_\nu \lambda_\nu \rangle = \langle \lambda'_1 \vec{q} \lambda'_2 -\vec{q} \alpha | A | 0 \vec{J}_\nu \lambda_\nu \rangle$$

The spiralities of residual particles in such Lorentz transformation are changed. However, further they will be summed up and the change will have no effect.

The relative decay probability of the channel λ (with the account of (II.5), is written as:

$$\frac{1}{\Gamma} g_{\lambda}^2 = \frac{q}{2\omega} \frac{1}{2J+1} \sum_{\lambda_1 \lambda_2} \int dC \frac{1}{4} \langle \lambda | \rho | \lambda \rangle$$

The amplitude A is normalized so that on summing the cross section over all particle channels we obtain the cross section of unstable particle production.

In the literature^[17] the density matrix of unstable particles in the axes system is usually considered as shown in Fig. 6 (the V-particle rest system).

The transition to this axes system is made by rotating the V-particle rest system:

$$\langle \lambda'_1 \vec{q} \lambda'_2 - \vec{q} a | \lambda | \theta | \lambda_{\nu} \lambda_{\nu} \rangle = \sum_M \langle \lambda' \vec{q} \lambda' - \vec{q} a | A | 0JM \rangle D_{M\lambda}^J(\omega)$$

This rotation takes the spin projection from the V particle momentum over to the pion momentum.

Introduce the density matrix:

$$\begin{aligned} \langle M' | \rho | M \rangle &= \frac{4\pi^2}{V E_{\pi} E_p} \frac{1}{2} \frac{P_a}{(E_{\pi} + E_p)} \sum_{\lambda_{\nu} \lambda_p \lambda'_p \lambda'_{\nu}} D_{M\lambda}^J(\omega) \langle \lambda_{\nu} J_{\nu} | R | \lambda_p P_p | E_{\pi} \rangle \times \\ &\times \langle \lambda_p P_p | E_{\pi} | R | \lambda_{\nu} J_{\nu} \rangle \langle \lambda' | \rho | \lambda' \rangle D_{M\lambda'}^J(\omega). \end{aligned}$$

The differential cross section of the V-particle production is written as:

$$\frac{d\sigma}{d\Omega} = S p \rho$$

Introduce also the normalized density matrix

$$\langle M' | \bar{\rho} | M \rangle = \frac{\langle M' | \rho | M \rangle}{S p \rho}$$

Using the introduced determinations the cross section of reactions (II.1) and (II.2) can be written as:

$$d\Omega_p d\Omega_q \sum_{MM'} \langle \lambda'_1 q \lambda'_2 - \vec{q}a | A | 0 JM' \rangle^* \langle M' | \rho | M \rangle \times \\ \lambda'_1 \lambda'_2 \\ \times \langle JM0 | A | \lambda'_1 \vec{q} \lambda'_2 - \vec{q}a \rangle \frac{q}{2m} f(m^2) dm^2,$$

where $f(m^2) = \delta(m^2 - m_2^2)$ or (II.6). Using Appendix I and the definition $\frac{\Gamma_a}{\Gamma}$ we find for the cross section

$$d\sigma_v d\Omega_q f(m^2) dm^2 \frac{q}{2m} \left(\frac{3}{4\pi} \right) \sum_{MM'} |A(\lambda_1, \lambda_2)|^2 e^{i(M-M')\Phi} \Phi_{d_{1M}}^j(\theta^*) d_{1M}^j(\theta^*) \times \quad (\text{II.7})$$

$$\langle \langle M' | \tilde{\rho} | M \rangle \rangle = d\sigma_v d\Omega_q \frac{\Gamma_a}{\Gamma} \frac{3}{4\pi} \frac{1}{2} [1 - w_{00}(\theta^*, \Phi)] f(m^2) dm^2.$$

APPENDIX III

Consider the contribution of (e^+e^-) -pairs produced in collisions of strongly interacting particles when this process does not go through the resonance state in the (e^+e^-) -channel.

In other words, consider the reaction

$$a + b \rightarrow c + d + \dots + e^+ + e^-, \quad (\text{III.1})$$

where a, b, c, \dots are any strongly interacting particles. The matrix element of process (III.1) is given as

$$M = J_\mu \frac{e^2}{t} \bar{u}(P_2) \gamma^\mu v(P_1), \quad (\text{III.2})$$

t is the four-dimensional momentum of the virtual photon ($t = P_1 + P_2$, where P_2 and P_1 are electron and positron momenta), $u(P_2), v(P_1), \gamma^\mu$ - spinors and Dirac matrices, J_μ - the operator, describing strong interactions. The differential cross section of process (III.1) can be written using formula (II.5):

$$d\sigma = \frac{4\pi^2}{VE_a E_b} \frac{1}{2} \prod_i \frac{d^3 P_i}{E_i} \frac{d^3 t}{t_0} \delta^4[\Sigma P_i + t - P_0] d\Omega_q \Sigma |M|^2, \quad (\text{III.3})$$

where P_i - momenta of particles of the final state expect and e^+, e^- . Integrating this expression over $d^3 t$ and $d^3 P_i$, passing over to $\vec{t} = 0$ and distinctly separating the dependence of M upon t , we find:

$$d\sigma = f \frac{dm}{m^6} \sqrt{m^2 - 4m_e^2}, \quad (\text{III.4})$$

where $m = 2\sqrt{m_e^2 + q^2}$, m_e is electron mass, f is the relativistically invariant function of the electron mass. The assumption that $f(m)$ has poles on m^2 corresponds to that on resonances in the e^+e^- -system and has been considered in Appendix II.

Consider the case when Γ is weakly dependent on m (there is no resonance in the (e^+e^-) -system, however, the processes of $\gamma^0 \rightarrow \pi^0 + e^+ + e^-$, $\pi^0 \rightarrow \gamma + e^+ + e^-$ refer to the case in question as these are resonances in another channel). From formula (III.4) it is seen that $d\sigma$ has a very sharp peak near $m = 2m_e$. The upper-limit of the number of pairs having the effective mass m larger than the given value M (to the total number of pairs, produced in process III.1) is written as

$$\frac{N(m > M)}{N_{\text{tot}}} = \left(\frac{2m_e}{m}\right)^3 \quad (III.5)$$

From formula (III.5) it is seen that with $m \geq 0.5$ GeV the contribution of the nonresonance (e^+e^-) pairs is negligibly small. This is also valid to such cases when the number of resonance pairs is considerably smaller than the total number of nonresonance pairs N_{tot} (for instance

$$\frac{N_{\text{tot}}(\omega \rightarrow \pi^0 + e^+ + e^-)}{N(\omega \rightarrow e^+ + e^-)} \approx 10).$$

R e f e r e n c e s

1. Y.Nambu and J.J.Sakurai. Phys.Rev.Lett., 8, 79 (1962).
2. M.Gell-Mann, D.Sharp and W.G.Wagner. Phys.Rev.Lett., 8, 261(1962).
3. R.F.Dashen and D.H.Sharp. Phys.Rev., 133, 7B 1585 (1964).
4. Е.Д. Жижин и В.В. Соловьев. ЖЭТФ 43, 268 (1962).
5. Нгуен Ван Хьеу и Фам Куи Ты. Препринт ОИЯИ Р-2338 (1965).
6. В.В. Бармин, А.Г. Долголенко, Ю.С. Крестников, А.Г. Мешковский, В.А.Шебанов. ЖЭТФ, 45, 6(12) 2082 (1963).
7. J.J. Murray, M.Ferro-Luzzi, D.O.Hiwe, I.B.Shafer, F.T.Solmitz, M.Lynn Stevenson. Phys.Lett., 7, 358 (1963).
8. A.Bozagaet, U.Nguyen-Khac, A.Rousset, A.Haatuft, A.Halsteinlid, R.S.Luechford, F.R. Stannard. Phys.Lett., 12, 70 (1964).
9. R.A.Zdanis, L.Madansky, R.W.Kraemer, S.Hertzbach, R.Strand. Phys. Rev.Lett., 11, 721 (1965).
10. D.M.Binnie, A.Duane, M.R.Jane, W.G.Jones, D.C.Mason, J.A.Newth, D.C.Potter, Ijaz Ur Rahman, J.Walters, B.Dickinson, R.J.Ellison, A.E.Harckham, M.Ibbotson, R.Marshall, R.F.Templeman, A.I.Wenroo. Phys.Lett., 18, 343 (1965).

11. М.А. Азимов, А.М. Балдин, В.С. Пантуев, Л.В. Сильвестров, М.Н.Хача-
турян, И.В. Чувило. Публикация ОИЯИ Б7-2070 (1965).
12. A.Benson, L.Lovell, C.T.Murphy, B.Roc, D.Sinclair, I.Vander-Velde.
Preliminary Version Submitted to the XIII th International Conf.
on High Energy Physics, Univ. California.
13. I.D.Jackson, I.T.Donohue, K.Gottfried, R.Keyser and B.E.Y.Svensson.
Phys.Rev., 139, B428 (1965).
14. М.А.Азимов, А.С.Белусов, I.V.Chuvilo, R.Firkowski, M.N.Khachatu-
ryan, M.S.Khvastunov, L.G.Makarov, E.I.Maltsev, A.T.Matyushin,
V.T.Matyushin, V.S.Pantuyev, L.N.Shtarkov, D.V.Uralsky, B.A.Zele-
nov, L.I.Zhuravleva. Preprint E13-2971, Dubna (1966).
15. M.Ross., L.Stodolsky. Preprint Univ. of Michigan. BNL 10146(1966).
16. M.Jacoba, G.C.Wick, Ann.Phys., 7, 404 (1959).
17. K.Gottfried, J.D.Jackson. Nuovo Cimento 33, 309 (1964).
18. S.Bergia, F.Binsignari and A.Stanghellini. Nuovo Cimento 16,1073(1960).
19. ABBBHLM. Collaboration. Nuovo Cimento 31, 729 (1964).
20. A.Weinmann, E.Engels, Jr.,L.N.Hand, C.M.Hoffmann, P.G.Innocenti,
Richard Wilson, W.A.Blanpied, D.I.Drickey and D.G.Stairs. Phys.
Rev.Lett., 17, 1113 (1966).
21. E.Shibata and M.Wahlig, Phys.Lett., 22, 354 (1966).

Received by Publishing Department
on January 31,1967.

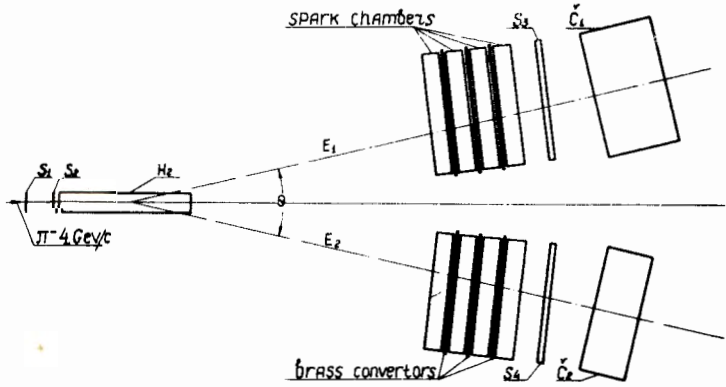


Fig. 1. Schematic view of the experimental arrangement and geometry. S_1, S_2, S_3, S_4 are scintillation counters. C_1, C_2 are Cerenkov total absorption gamma-spectrometers. H_2 is a liquid hydrogen target 50 cm long.

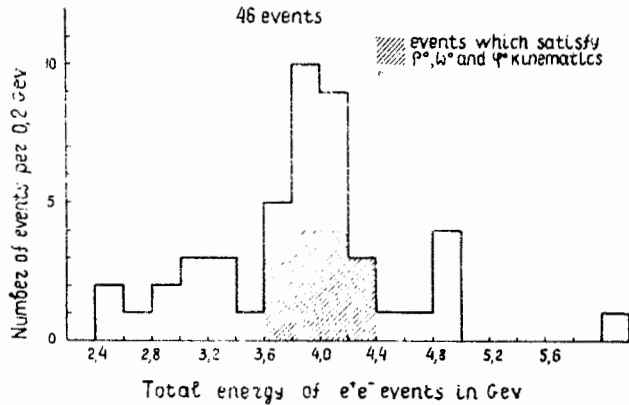


Fig. 2. Sum distribution of the energy ($E_1 + E_2$) for 46 events. For the further analysis the events were taken whose total energy was in the energy range $3.6 < (E_1 + E_2) < 4.4$ GeV and $E_1 > 0.5$ GeV, $E_2 > 0.5$ GeV.

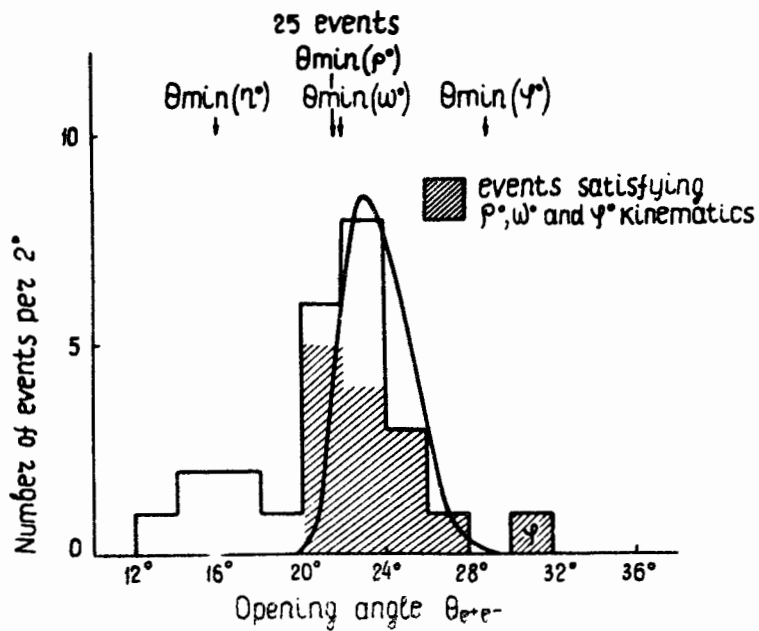


Fig. 3. Opening angle distribution for 25 events for ρ° and ω° kinematics according to spark chamber pictures and ψ° to total energy. The continuous curve is a theoretical one calculated for ρ° kinematics.

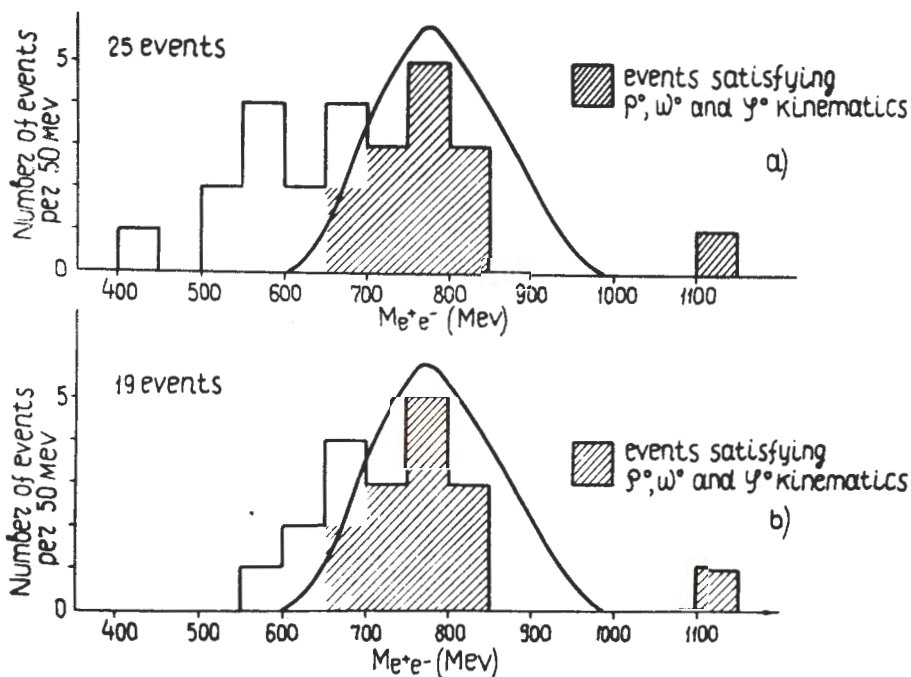


Fig. 4. Effective mass distributions for a) 25 candidates for e^+e^- -pairs selected according to spark chamber pictures and to their total energy; b) 19 candidates for e^+e^- -pairs selected; 1) according to spark chamber pictures: a single track of the charged particle in spark chambers of the first and second channels, 2) according to their energy: $E_1 > 0.5$ GeV; $E_2 > 0.5$ GeV and $3.6 < (E_1 + E_2) < 4.4$ GeV, 3) according to the opening angle $\theta_{e^+e^-} > 20^\circ$ (in the lab.system). Continuous curve is a theoretical one calculated for ω -mesons.

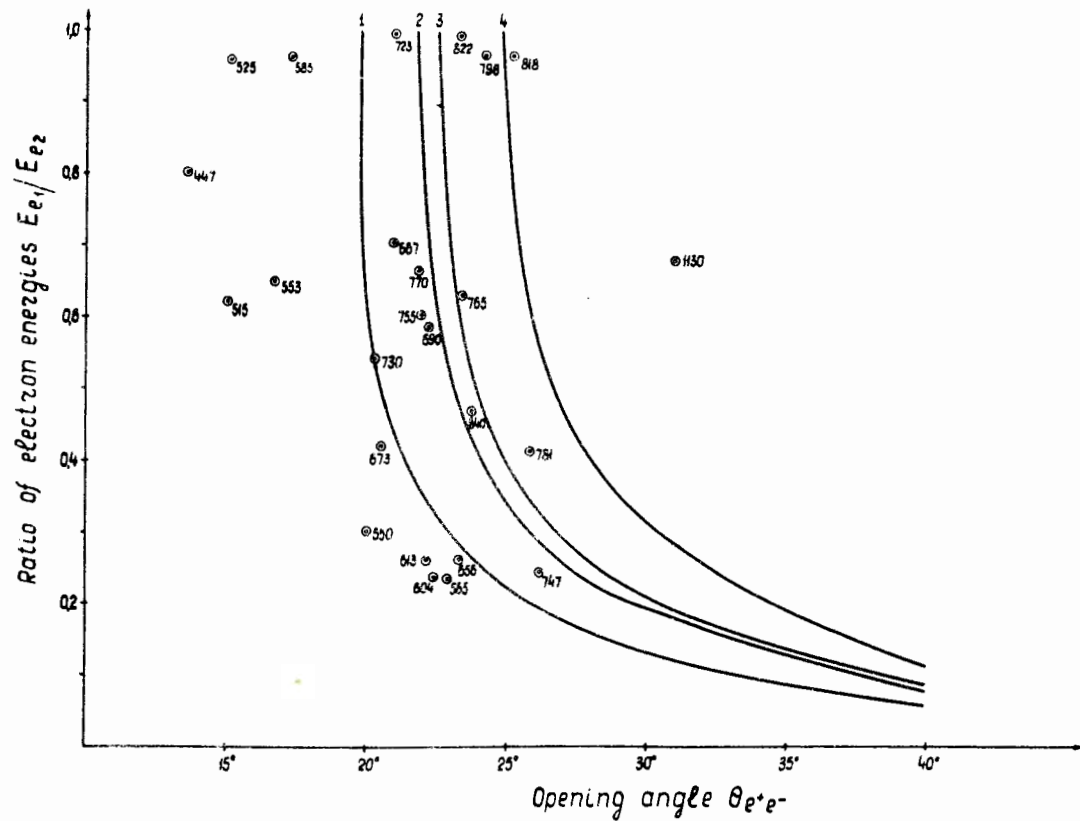


Fig. 5. Dependence of the decay particle energy ratio E_{e_1}/E_{e_2} upon the opening angle $\theta_{e^+e^-}$ (in the labels in degrees). Curves 2 and 3 are theoretical ones calculated for 1.0 GeV p and ω -mesons. Curves 1 and 4 show the boundaries for absorption curves 2 and 3 corresponding to two standard deviations for the energy and angular resolutions of the apparatus.

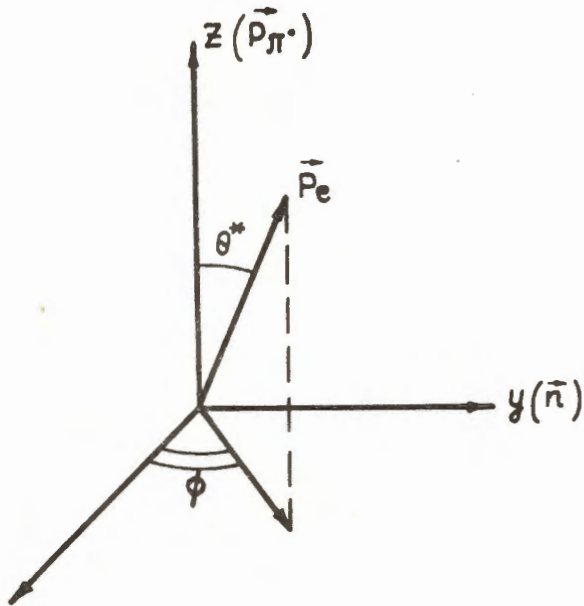


Fig. 6. The direction of the coordinate axes in the rest system of the decaying particle.

Наблюдение (e^+e^-) -распадов нейтральных векторных мезонов

С помощью системы совместно работающих вакуумных камер и черенковских γ -спектрометров полного поглощения измерены сечения образования (e^+e^-) -пар в реакции: $e^+p \rightarrow V^0 + e^+ \nu^+ e^- \bar{\nu}^-$ при $P = 4,0$ ГэВ/с. В отличие от ранее применявшегося метода установки могла измерять как углы распада, так и энергии продуктов распада V^0 -частицы, и, следовательно, возможна составлять в каждом событии ее эффективную массу. Обнаружено 13 событий, идентифицированных как распады: $\omega^0 \rightarrow e^+e^-$ и $\rho^0 \rightarrow e^+e^-$ и одно событие: $\phi^0 \rightarrow e^+e^-$.

Из полученных сечений и известных из литературы сечений образования ω^0 , ρ^0 и ϕ^0 -мезонов сделано для независимых определений ширины распада октета векторных мезонов на e^+e^- :

$$\Gamma(V_8 \rightarrow e^+e^-) = (0,46 \pm 0,14) \cdot 10^{-2} \text{ МэВ}$$

$$\Gamma(V_8 \rightarrow e^+e^-) \leq 2,6 \cdot 10^{-2} \text{ МэВ}$$

что соответствует отношениям вероятностей:

$$\frac{\Gamma(\phi^0 \rightarrow e^+e^-)}{\Gamma(\rho^0)} = (0,39 \pm 0,12) \cdot 10^{-4}; \quad \frac{\Gamma(\omega^0 \rightarrow e^+e^-)}{\Gamma(\omega^0)} = (0,46 \pm 0,18) \cdot 10^{-4};$$

$\frac{\Gamma(\phi^0 \rightarrow e^+e^-)}{\Gamma(\omega^0)} \leq 2 \cdot 10^{-3}$. Для угла $\theta = \phi$ измерения было использовано значение $\theta = 38^\circ$.

Препринт Объединенного института ядерных исследований, Дубна, 1967.

Observation of the (e^+e^-) -Decay Modes of Neutral Vector Mesons

The cross sections of (e^+e^-) pair production have been measured in the reactions $\pi^- + p \rightarrow V^0 + n$, $V^0 \rightarrow e^+e^-$ at $P=4.0$ GeV/c using a system of jointly operating spark chambers and Cerenkov total absorption γ -spectrometers. In contrast to earlier techniques our apparatus made it possible to measure both the opening angles and the energies of the V^0 -particle decay products and, hence, to determine its effective mass in each event. 13 events were detected and identified as the $\rho \rightarrow e^+e^-$ and $\omega \rightarrow e^+e^-$ decays and one $\phi \rightarrow e^+e^-$ event.

From the cross sections obtained and total cross sections for ρ , ω and ϕ -mesons known from the literature two independent determinations of the width of the vector meson octet decay into e^+ and e^- have been made: $\Gamma(V_8 \rightarrow e^+e^-) = (0.45 \pm 0.14) \cdot 10^{-2}$ MeV; $\Gamma(V_8 \rightarrow e^+e^-) \leq 2.6 \cdot 10^{-2}$ MeV, which corresponds to probability ratios: $\frac{\Gamma(\rho \rightarrow e^+e^-)}{\Gamma(\rho)} = (0.39 \pm 0.12) \cdot 10^{-4}$; $\frac{\Gamma(\omega \rightarrow e^+e^-)}{\Gamma(\omega)} = (0.46 \pm 0.15) \cdot 10^{-4}$
 $\frac{\Gamma(\phi \rightarrow e^+e^-)}{\Gamma(\phi)} \leq 2 \cdot 10^{-3}$. The value $\theta = 38^\circ$ was used for the ω - ϕ mixing angle.